NUMERICAL METHOD TO PHOTOELASTICITY USING PLANE POLARISCOPE

Caio Nelson Nogueira Napoles (caionapoles@gmail.com)

Ana Laura Mendonça Almeida Magalhães (almam2000@gmail.com)

Pedro Américo A. M. Júnior (pamerico@pucminas.br)

Filipe Gomes Vieira (filipevieira_90@hotmail.com)

João Leonardo Ribeiro Neto (joaoneto@pucminas.br)

Pontifícia Universidade Católica de Minas Gerais

Av. Dom José Gaspar, 500, Coração Eucarístico, Belo Horizonte, Minas Gerais, Brasil – 30535-610.

Abstract: *This research has the aim to find a new way to get the intensity equations for the phase-shifting model in digital photoelasticity. The procedure is based on the rotation of the analyzer itself. From the intensity equations, the isoclinic and isochromatic equations parameters are deduced by applying a new numerical technique. This approach can be done to calculate how many images allow the resolution of the polariscope. Each image indicates the stress forces in the object. In this study the plane polariscope was used. The amount of images will determinate the number of errors and uncertainties of the study, due to the observation that the veracity of the equations increases considerably with a large amout of images. Several analyses are performed with different amounts of photographic images. The results showed the possibility to measure stress forces with high precision using plane polariscopes.*

Keywords: *Phase shift; Optical instruments; Phase measurement; Birefringence; Polarization.*

1 INTRODUCTION

In phase-shifting algorithms, the change in phase is achieved by rotation of the optical elements of the polariscope. This requires that all optical elements in polariscope are able to rotate independently. Unfortunately, this is not the case for many commercially available polariscopes widely used in laboratories of industries and universities. The significant advantage of the methodology proposed in this study is that the method only changes the angle of the analyzer in the polariscope and based on that, it is possible to obtain equations for calculating the phase for any number of images in various situations. The physical reason for the proposed numerical model is based on the fact that the measurement uncertainty can be reduced by increasing the number of observations. This new method can be used with any number of photographic measures and in any plane polariscope. Plane polariscope based algorithms give better isoclinic values than the methods that use a circular polariscope. The advantage is its immunity to mismatch with the quarter-wave plate. The isochromatic data evaluated with algorithms based on plane polariscope are accurate, although the unwrapping process of isochromatic data is most difficult. With better results in isoclinic and isochromatic analysis, it is possible to obtain less errors in separation of stresses by the shear difference technique. For this reason, it is important to improve the technique elaborated for circular polariscopes and extend it for plane polariscopes. In this research, a new numerical model is suggested to overcome the limitation of the commercial polariscopes. A comparative study was made among the theoretical results and the numerical methodologies.

As the name implies, photoelasticity was developed to apply optical (photo) principles to solve engineering problems of elasticity. The method relies on the birefringence property exhibited by transparent plastics. In particular, the phenomenon of stress (or load) induced birefringence is utilized where the material becomes birefringence under the influence of external loading. The phenomenon was first observed by David Brewster in the early nineteenth century in glass and he foresaw the potential of this for stress analysis. However, glass was far from the ideal material although photoelasticity of glass has generated great interest. The technique was , however , systematically developed into a viable experimental stress analysis tool only in the second quarter of this century. The potential of 3-D stress analysis was also developed and to this day remains one of the very few experimental methods for 3-D stress analysis. With this background, photoelastictiy found widespread application in many industrial applications. In particular, determination of stress concentration in front of notches and holes was and still is one of the premier forte of photoelasticity in design of machine elements.

In the past two decades, photoelasticity has been overrun by the Finite Element Method (FEM). The simplicity and black box nature of FEM was particularly inviting to designers who did not have to get their hands dirty. However, while one cannot ignore the power of FEM, one has to realize the limitations of the method in it being as good as the model used. Indeed, critics of photoelasticity did mention that photoelasticity requires a birefringent model to be used instead of the actual structure. The same applies to FEM since it relies on a numerical model of the actual structure and loading to generate the stress and displacement distribution patterns. A new school of thought is the use of hybrid methods where advantages of both experimental and numerical methods are exploited. Nevertheless, recent needs such as continuous on-line monitoring of structures, residual stresses in glass (plastics) and microelectronics material , rapid prototype products and dynamic visualization of stress waves have brought photoelasticity into the limelight once again.

2 THE PHASE-SHIFTING METHOD

The plane polariscope is one of the simplest optical arrangements possible in photoelastic technique. The figure 1 shows the typical arrangement, when P, R and A represent polarizer, retarder (stressed model) and analyzer, respectively. The subscripts written after P and A mean the angle between the polarizing axis and the reference axis x. $P_\alpha R_{\theta,\delta} A_\beta$ indicate that the polarizer is at angle α and the analyzer is at an arbitrary angle β, both related with the x-axis as well. The subscripts δ and θ of R indicate the retardation added by stressed sample and whose fast axis is at angle θ with x-axis.

The output intensity given from the analyzer of the polariscope arrangement $P_\alpha R_{\theta,\delta} A_\beta$ is given by:

$$I = I_o\left[\left(\cos\frac{\delta}{2}\right)^2\left(\cos(\beta-\alpha)\right)^2 + \left(\sin\frac{\delta}{2}\right)^2\left(\cos(\beta+\alpha-2\theta)\right)^2\right]. \tag{1}$$

where Io accounts for the amplitude of vector of the incident light and also the constant of proportionality and I represents the light intensity.

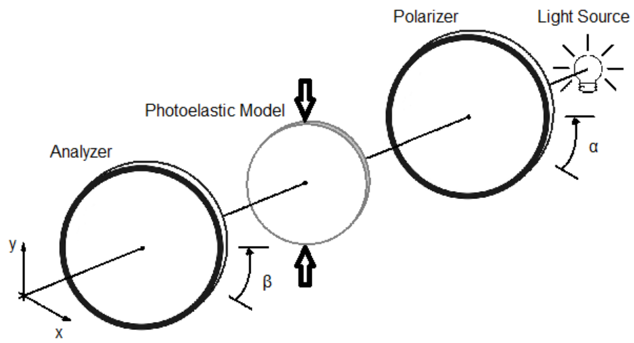

Fig. 1. Optical arrangement of a plane polariscope.

In the experimental procedure, the diameter and the thickness of the disk are D = 50 mm and t = 15 mm, respectively. An diametrically opposite load, P = 50 N is applied on disk. An epoxy resin with stress fringe value F = 4.85 N/mm/fringe was used. In photoelastic analysis, the theoretical value of isochromatic δ is related to two principal stress components, σ_1 and σ_2, as in Eq. (2). The theoretical isoclinic angle θ can be calculated using Eq. (3) with stress components σ_x, σ_y and τ_{xy}.

$$\delta = \frac{2\pi t}{F}(\sigma_1 - \sigma_2). \tag{2}$$

$$\theta = \frac{1}{2}\tan^{-1}\left(\frac{2\tau_{xy}}{\sigma_x - \sigma_y}\right). \tag{3}$$

Thus, using Eqs. (2) and (3), the exact value of δ and θ can be calculated for each point of the disk. Then, the experimental measurements of δ and θ, obtained from the proposed method in this research, is compared with its exact values in order to validate the new equations.

3 THE PROPOSED MODEL

Using the same principle of the mathematical model proposed in [1,5,15,16,17], a new model for the phase equations is developed by the comparison with the conventional form for plane polariscopes. The general equation to calculate the photoelastic parameters with any number (N) of images is proposed:

$$\theta = \frac{1}{2}\tan^{-1}\left(\frac{\sum_{j=1}^{N} b_j I_j}{\sum_{j=1}^{N} c_j I_j}\right). \tag{4}$$

$$\delta = \cos^{-1}\left(\frac{\cos 2(\theta-\alpha)\left(\sin 2\theta\sum_{j=1}^{N} d_j I_j + \cos 2\theta \sum_{j=1}^{N} e_j I_j\right)}{\sin 2(\theta-\alpha)\left(\cos 2\theta\sum_{j=1}^{N} f_j I_j + \sin 2\theta \sum_{j=1}^{N} g_j I_j\right)}\right). \tag{5}$$

where N is the number of images, b_j, d_j and e_j are the coefficients of numerator, c_j, f_j and g_j are coefficients of denominator, and j is the index of the sum. A mathematical model was obtained as shown in Eq. (4) for isoclinic angle θ and in Eq. (5) for isochromatic parameter δ.

The mathematical model is easy to be solved for the fact that it involves a linear programming and a maximization. Both can be obtained using the Simplex Methods. The processing time to solve those equations, even using personal computers, is considerably fast, taking a few seconds to be completed.

The shift from obtaining equations for calculating the phase analytically to obtain them numerically is a significant innovation. It breaks a paradigm that was hitherto used by several authors [6-13]. After several attempts, the following mathematical model was identified to solve the problem numerically:

$$\begin{array}{ll} \textit{Maximize} & \sum_{j=1}^{N} b_j + c_j \\ & \\ \textit{subject to} & \left\{\begin{array}{lll} & & \textit{Quantities} \\ 1) & \tan(2\theta^{\nu})\sum_{j=1}^{N} c_j . I_j^{\nu} = \sum_{j=1}^{N} b_j . I_j^{\nu} & \nu > 2N \\ 2) & -1 \le b_j \le 1, \quad -1 \le c_j \le 1 & j = 1..N \\ 3) & b_j,\ c_j \ \textit{are real numbers} & j = 1..N \end{array}\right. \end{array} \tag{6}$$

$$\begin{array}{ll} \textit{Maximize} & \sum_{j=1}^{N} d_j + e_j + f_j + g_j \\ & \\ \textit{subject to} & \left\{\begin{array}{lll} & & \textit{Quantities} \\ 1) & \begin{array}{c} \cos(\delta^{\nu})\sin[2.(\theta^{\nu}-\alpha)].\left[\cos(2.\theta^{\nu}).\sum_{j=1}^{N} f_j . I_j^{\nu} + \sin(2.\theta^{\nu}).\sum_{j=1}^{N} g_j . I_j^{\nu}\right] = \\ \cos[2.(\theta^{\nu}-\alpha)].\left[\sin(2.\theta^{\nu}).\sum_{j=1}^{N} d_j . I_j^{\nu} + \cos(2.\theta^{\nu}).\sum_{j=1}^{N} e_j . I_j^{\nu}\right] \end{array} & \nu > 4N \\ 2) & -1 \le d_j \le 1, \quad -1 \le e_j \le 1, \quad -1 \le f_j \le 1, \quad -1 \le g_j \le 1 & j = 1..N \\ 3) & d_j,\ e_j,\ f_j,\ g_j \ \textit{are real number} & j = 1..N \end{array}\right. \end{array} \tag{7}$$

$$\left\{\begin{array}{l} I_j^v = I_o^v.\left[\cos^2\left(\frac{\delta^v}{2}\right).\cos^2\left(\beta_j - \alpha\right) + \sin^2\left(\frac{\delta^v}{2}\right).\cos^2\left(\beta_j + \alpha - 2.\theta^v\right)\right], j = 1..N \\ I_o^v \in [0;\ 255]\quad random\quad and\quad real \\ \theta^\upsilon \in \left[-\pi/4,\ \ \pi/4\right]\quad random\quad and\quad real \\ \delta^\upsilon \in \left[0,\ \ \pi\right]\quad random\quad and\quad real \\ \beta_j = \left[(\ UpperAngle\ - LowerAngle\ )\frac{\pi(j-1)}{180(step-1)} + \pi\frac{LowerAngle}{180}\right], j = 1..N \end{array}\right.$$

$$\begin{array}{l} step = divisors\ (\ UpperAngle\ - LowerAngle\ ) + 1 \\ \text{step is increase the angle of the analyzer (Integer in degrees)} \\ N = \text{number of images from 3 until the step value (Integer)} \\ j = 1..N \\ \beta_j = \text{analyzer angle} \\ \alpha = \text{polarizer angle} \\ \theta = \text{isoclinic angle} \\ \delta = \text{isochromat ic parameter} \\ \text{LowerAngle} = \text{Lower angle analyzer in degrees (Integer)} \\ \text{UpperAngle} = \text{Upper angle analyzer in degrees (Integer)} \\ \text{Input: LowerAngle, UpperAng le and } \alpha \\ \text{Output: For each value of N and step: } \mathrm{b_j, c_j, d_j, e_j, f_j} \text{ and } \mathrm{g_j} \text{ with } \mathrm{j = 1..N} \end{array} \qquad (8)$$

The mathematical models above maximize the coefficients of numerator (b_j, d_j, e_j) and the coefficients of denominator (c_j, f_j, g_j) in both equations, thus the obtained values for them are large enough to be significant in Eqs. (4) and (5). The Step represents the increasing angle of the analyser and has values greater than two. N is the number of images and an integer number between three and the value of the step.

The constraints 1 in Eqs. (6) and (7) are made so that all coefficients generate correct values for the calculation of θ and δ. To ensure that one has a hyper-restricted problem, suggest that the number of greater restrictions must have be least equal with the number of variables. The constraints 2 and 3 in Eqs. (6) and (7) indicate that the coefficients are real numbers with values between one and minus one. With these procedures, the error propagation is avoided. For the evaluation phase, these limiting factors will increase the values of intensity I_o that contains errors due to noise and improve discretization in pixels and in shades of gray 1. In the model, the values of Io is limited between 0 and 255, θ is limited between $-\pi/4$ and $\pi/4$ and δ is limited between 0 and π. The analyzer angle β is an integer number which varies from 0° to 90°. The *step* defines the distance between the angles adjusted in the analyzer, for instance, a value *step* = 4 gives four images with β equally spaced from 0° to 90°, if N = 4 the four images are used, if N = 3 only the three first images are used. Table 1 shows the coefficients for N = 4, *step*= 4, α = 90° and the angles of the analyzer (β) as follows: 0°, 30°, 60°, 90°. Table 2 shows the coefficients for N = 3, *step* = 4, α = 90° and the angle β as follows: 0°, 30°, 60º.

Table 1. Values of the real coefficients (b_j, c_j, d_j, e_j, f_j, g_j) when N = 4 and *step* = 4

j	β_j	b_j	c_j	d_j	e_j	f_j	g_j
1	0°	0.00000	1.00000	0.79904	1.00000	1.00000	-0.68301
2	30°	0.52360	1.00000	-0.73205	1.00000	1.00000	0.57735
3	60°	1.04720	-1.00000	-1.00000	-0.69060	-1.00000	1.00000
4	90°	1.57080	-0.50000	0.93301	0.26795	0.63397	-0.89434

Table 2. Values of the real coefficients ($b_j, c_j, d_j, e_j, f_j, g_j$) when N = 3 and *step* = 4

j	β_j	b_j	c_j	d_j	e_j	f_j	g_j
1	0°	0.00000	0.66667	-1.00000	0.19936	1.00000	-0.48803
2	30°	0.52360	-1.00000	1.92265	1.00000	-0.57735	0.73205
3	60°	1.04720	0.33333	0.07735	-0.33333	0.57735	-0.24402

To verify the new equations for the calculating phase, a computer program that generated random values of I_o, θ and δ was created. With Eq. (1) are calculated N values of I_j to each value of β_j, then the new phase equations were applied on the values of I_j to determine whether they produced correct values of θ and δ. The calculations of the accuracy were performed thousands of times (at least 100000 times) for each equation in phase calculation. At least 99.999% of the times, we obtain the accuracy ($\left|\theta^{random} - \theta\right| \left|\delta^{random} - \delta\right|) \leq 10^{-6}$. The models of Eqs. (4) and (5) were tested until *step* and N equal to 2000, the value at which the increment $\Delta\beta$ would be 0.05°. This numerical test was performed to evaluate the capability of Eqs. (4) and (5) calculate correct values for θ and δ from intensity values.

To evaluate the performance of the Eqs. (4) and (5) in photoelastic analysis, an experiment was performed using a disk under diametral compression, a pixel number of M = 1024 x 1024 in the digitization, a grey level between 0 and 255 and a white light source. Figure 2 shows a flowchart of processing to phase-shifting method applied.

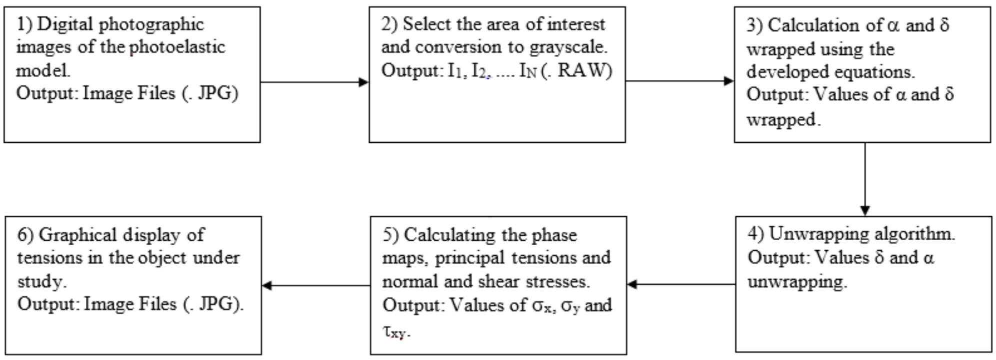

Fig. 2. Flowchart showing each processing stage.

The new equations were tested in the experimental procedures using a disk under diametral compression whose exact solution is known. Thus, using Eqs. (9) and (10), it was possible to evaluate the average relative error by comparing the experimental and exact results.

$$E_\theta = \frac{1}{M}\sum_{i=1}^{M}\frac{\left|\theta_i^{exact} - \theta_i\right|}{\left|\theta_i^{exact}\right|}. \quad (9)$$

$$E_\delta = \frac{1}{M}\sum_{i=1}^{M}\frac{\left|\delta_i^{exact} - \delta_i\right|}{\left|\delta_i^{exact}\right|}. \quad (10)$$

Where E_θ and E_δ represent the average relative error for θ and δ, respectively. M is the number of pixels of the image and θ_i^{exact} and δ_i are the exact values, calculated by the theory of elasticity. θ_i and δ_i are calculated using Eqs. (4) and (5). This comparison process was made for a number of images between 3 and 46.

4 RESULTS AND DISCUSSION

The results calculated with the Eqs. (4) and (5) were compared with the analytical solution for the disk under compression using the equations (9) and (10). We used fourty-four images (*N* from 3 to 46) and *step* values of 4, 5, 6, 7, 10, 11, 13, 16, 19, 21, 31, 37 and 46 were considered. The results obtained from Eqs. (9) and (10) are plotted in figure 3. The data in figure 3 show that the average error decreases when the number of images increases. It was also noted that for a same number of images, the average error increases when the variation of the angle β between the images decreases. The possible origins of this trend is unknown.

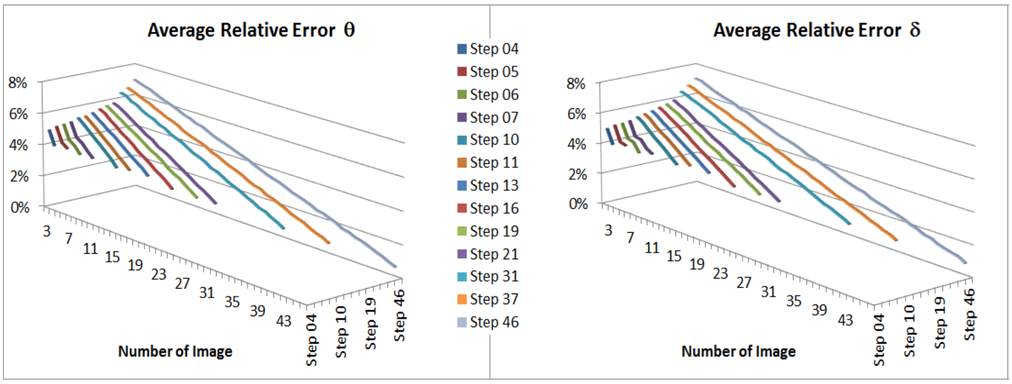

Fig. 3. Average error of θ and δ.

After obtained unwrapped values of θ and δ [17,18], it was applied in the shear difference technique for whole field stress separation. Both normal and shear stress were estimated. The figure 4 shows the results obtained with the application of the new phase calculation equations, using N = 4 and step = 4.

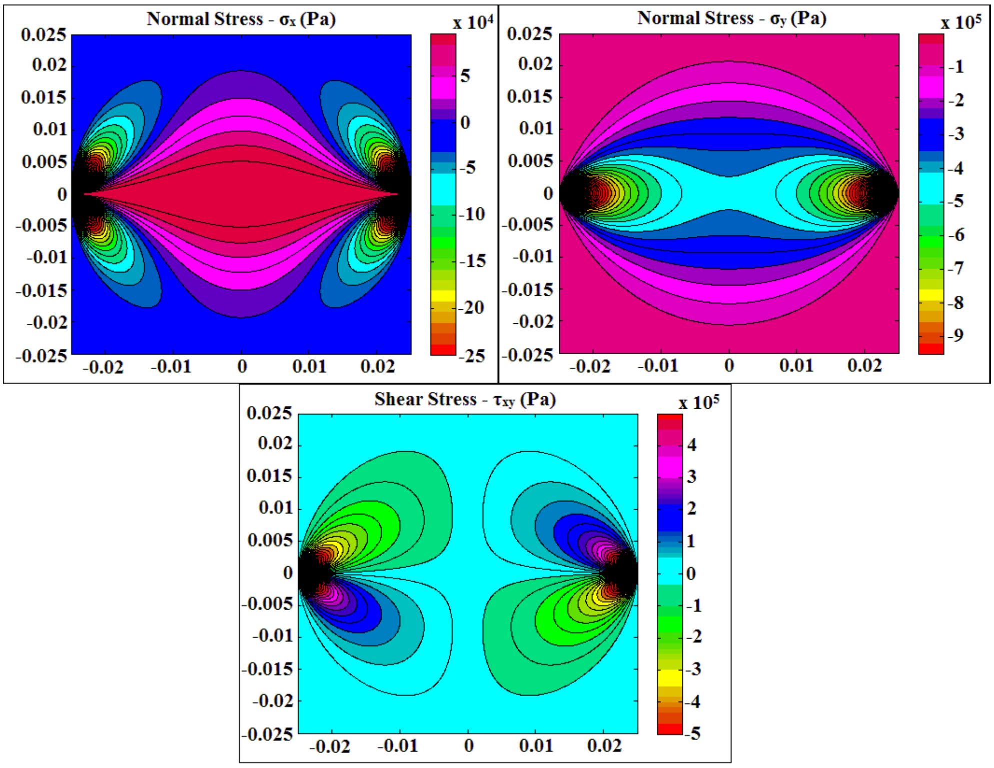

Fig. 4. Results obtained through experimental measurements using the new equations with N = 4 and *step* = 4 of: σ_x, σ_y, τ_{xy}.

5 CONCLUSION

In this study a simpler numerical model for plane polariscope using the phase-shifting technique with numerical equations for the calculation of phase was developed. It was concluded that increasing the number of images, the average error decreases, which is an advantage over the conventional method. The main advantage of this numerical approach over the conventional method is its versatility, due to the fact that it could be used in any commercially available polariscope, eliminating the need for dedicated equipment to determine experimental photoelastic parameters. Furthermore, the new method facilitates the automation of the analysis; now only the analyzer is rotated to collect the photographic images. The results of the research indicates that the method provides small errors, being applicable to experimental stress or strain analysis. It was observed that by increasing the number of images there is a linear rate tendency of reduction of relative error in stress measurements.

REFERENCES

C. A. Magalhães and P. A. A. Magalhães Júnior, “New numerical methods for the photoelastic technique with high accuracy,” J. Appl Phys. 112, 083111 (2012).

M. Ramji., K. Ramesh, “Whole field evaluation of stress components in digital photoelasticity – issues, implementation and application,” Opt. Lasers Eng. 46(3), 257-271 (2008).

K. Gallo and G. Assanto, "All-optical diode based on second-harmonic generation in an asymmetric waveguide," J. Opt. Soc. Am. B 16(2), 267–269 (1999).

J. A. Quiroga and A. González-Cano, "Method of error analysis for phase-measuring algorithms applied to photoelasticity," Opt. Express 37(20), 4488–4495 (1998).

K. Ramesh, Digital Photoelasticity: Advanced Techniques and Applications (Springer-Verlag, 2000).

C. Fang, Y. Xiang, K. Qi, C. Zhang, and C. Yu, "An 11-frame phase shifting algorithm in lateral shearing interferometry," Opt. Express 21, 28325-28333 (2013).

F. Liu, Y. Wu, and F. Wu, "Phase shifting interferometry from two normalized interferograms with random tilt phase-shift," Opt. Express 23, 19932-19946 (2015).

L. Fei, X. Lu, H. Wang, W. Zhang, J. Tian, and L. Zhong, "Single-wavelength phase retrieval method from simultaneous multi-wavelength in-line phase-shifting interferograms," Opt. Express 22, 30910-30923 (2014).

O. Medina, J. C. Estrada, and M. Servin, "Robust adaptive phase-shifting demodulation for testing moving wavefronts," Opt. Express 21, 29687-29694 (2013).

Y. Du, G. Feng, H. Li, J. Vargas, and S. Zhou, "Spatial carrier phase-shifting algorithm based on principal component analysis method," Opt. Express 20, 16471-16479 (2012).

H. Guo and B. Lü, "Phase-shifting algorithm by use of Hough transform," Opt. Express 20, 26037-26049 (2012).

C. Robledo-Sanchez, R. Juarez-Salazar, C. Meneses-Fabian, F. Guerrero-Sánchez, L. M. A. Aguilar, G. Rodriguez-Zurita, and V. Ixba-Santos, "Phase-shifting interferometry based on the lateral displacement of the light source," Opt. Express 21, 17228-17233 (2013).

F. Liu, Y. Wu, and F. Wu, "Correction of phase extraction error in phase-shifting interferometry based on Lissajous figure and ellipse fitting technology," Opt. Express 23, 10794-10807 (2015).

M. Ramji, V. Y. Gadre and K. Ramesh, "Comparative study of evaluation of primary isoclinic data by various spatial domain methods in digital photoelasticity", J. Strain Anal. Eng. 41(5), 333-348, 2006.

M. Ramji and K. Ramesh, "Whole field evaluation of stress components in digital photoelasticity – Issues, implementation and application", Opt. Lasers Eng. 46, 257-271, 2008.

M. Ramji, and R. G. R. Prasath, "Sensivity of isoclinic data using various phase shifting techniques in digital photoelasticity towards generalized error sources", Opt. Lasers Eng. 49, 1153-1167, 2011.

N. Plouzennec and A. Lagarde, "Two-wavelengh method for full-field automated photoelasticity", Exp. Mech. 39(4), 274-277, 1999.

P. Pinit, and E. Umezaki, "Absolute fringe order determination in digital photoelasticity", JSMME, 2(4), 519-529, 2008.